

Mechanical properties of glass fibre reinforced polypropylene disks produced by rotating, expansion and compression injection moulding

Cristina A. Silva · Júlio C. Viana ·
Ferrie W. J. van Hattum · António M. Cunha

Received: 23 March 2006 / Accepted: 15 June 2006 / Published online: 23 February 2007
© Springer Science+Business Media, LLC 2007

Abstract A special mould (RCEM, rotation, compression and expansion mould) intended for inducing complex stress fields during the filling stage of injection moulding was used to manipulate the microstructure of a short fibre reinforced polypropylene. Centred gated discs were injection moulded with different filling sequences (stationary, expansion, compression, expansion with continuous rotation and compression with continuous rotation). The mechanical behaviour of the mouldings was characterized in tensile and flexural loadings on specimens cut at different locations along the flow length. Complete discs were also tested in 4-point support flexural test at low velocity and at impact. The respective results are analysed and discussed in terms of the developed fibre orientation morphology.

Introduction

In thermoplastics reinforced with glass fibres, the principal aim is to produce materials with better thermo and mechanical properties than those of the non-reinforced polymers. It is well known that glass fibres become oriented in the injection moulding process and that this orientation can have a pronounced effect on mechanical properties. Many authors [1–9] have

reported and discussed the effects of fibre orientation and/or fibre length distributions on the mechanical performance of injected mouldings. The composite is stronger and stiffer in the principal fibre orientation direction and weaker in the transverse direction. However, the fibre orientation is strongly influenced by the material flow during the moulding process and the geometric shape of the mould cavity. In fact, when a short-fibre reinforced polymer is injection moulded, the flow during mould filling develops preferential fibre orientation patterns in the part. As, each fibre is displaced its orientation changes as a function of the developed stress field, the polymer matrix, the interactions with other fibres and the mould surfaces. The result is a complex fibre orientation distribution, which varies considerably from one point to another—in particular across the moulding thickness. This fibre orientation pattern is the one dominant structural feature of a fibre reinforced composite [10].

In injection moulding, both shear and extensional dominated flows develop through the thickness and along the flow path. Shearing flows align fibres in the direction of flow and stretching flows tend to align fibres in the direction of the stretching [11]. For a centre-gated disc, the stretching axis is perpendicular to the radial flow direction, RFD. During injection moulding of a centre-gated disc, the shear dominated flow near the mould surfaces tends to align the fibres along RFD (skin region), whereas if the flow is extensional in the plane of the part, near the mid-plane of the cavity, the fibres tend to align transversely to RD (core region) [12–17].

In conventional injection moulding the possibilities of controlling the stress levels imposed to the melt during processing are very limited, for a fixed moulding

C. A. Silva · J. C. Viana (✉) · F. W. J. van Hattum ·
A. M. Cunha

Department of Polymer Engineering, University of Minho,
Campus de Azurém, 4800-058 Guimarães, Portugal
e-mail: jcv@dep.uminho.pt

geometry and material type. Within this scope an entirely new design of a special mould was developed, which allows for a wide variation of the flow and packing conditions in a flat disc geometry, assuring the manipulation of the stress fields developed in injection moulding [18–20]. One of the cavity walls (the ejection side) can rotate (clock and anticlockwise) and move with a linear movement (forward and backward) during the injection and holding stages. Two electric servomotors are used to directly drive those movements. This constructive solution enables to program different moulding sequences in the so-designated rotation, compression and expansion mould (RCEM) tool, with the in process variation of the cavity thickness and the rotation of one of its surfaces. A schematic representation of the cross-section view of the mould and the respective operating modes are presented in Fig. 1. A detailed description of this moulding tool can be found elsewhere [21].

The thermomechanical conditions imposed by RCEM dramatically influences the fibre alignment, changing the orientation profile of the reinforcements within the mouldings. A detailed description of the effect of linear (convergent and divergent) flow combined or not with rotation motion on the through-thickness distribution of fibre orientation in injection moulding of a centre-gated disc can be found elsewhere [22]. These active mould actions can be used to change the fibre orientation distribution from random to preferentially align.

Following this approach and using the above referred tool, the purpose of this paper is to analyse the effects of fibre orientation in the RCEM mould, by

considering distinct filling sequences (stationary, compression, expansion and compression and expansion combined under continuous rotation—Fig. 1) on the mechanical properties of glass fibre reinforced polypropylene mouldings.

Experimental

Materials and processing

The polymer used is a commercial grade of a 20% glass fibre reinforced polypropylene, Scolefin PP52G13-0 (melt flow index of 16 g/10 min, 230 °C/2.16 kg). Discs were injected in the RCEM with distinct filling sequences. Stationary plate mouldings were moulded with 1.0 mm and 4.0 mm of thickness for comparison purposes. During the filling stage, compression and expansion modes were used to produce convergent and divergent flows, respectively. The effect of the rotation action of the cavity plate combined under compression and expansion modes was also analysed.

The processing program was based on a fixed adjustment of the main processing variables (melt temperature of 230 °C; mould temperature of 20 °C, holding pressure (at screw tip) of 20 MPa and injection flow rate of 5 and 9 cm³/s for thinner and thicker mouldings, respectively). The RCEM set-up moulding conditions used are presented in Table 1. The mouldings were produced in a Ferromatik Milacron K85 injection moulding machine. The mould movements (variations of the linear and rotation motions) were adjusted as follows:

Fig. 1 Schematic moulding cavity and RCEM operating modes (the conditions studied in this work are in bold shade)

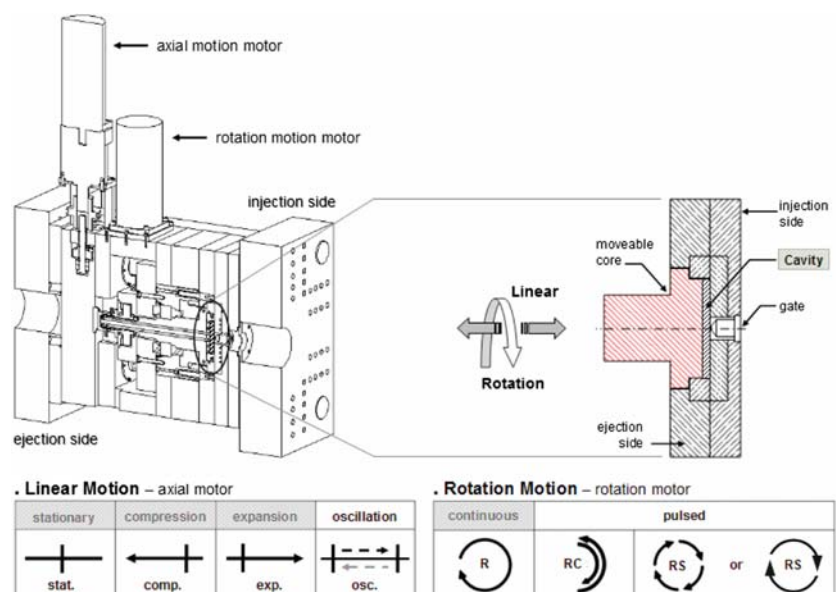


Table 1 RCEM set-up moulding conditions

References	RCEM—operating modes	
Stat.-1 mm	Linear motion Linear mode: <i>stationary</i> Cavity thickness: 1.0 mm	
Stat.-4 mm	Linear motion Linear mode: <i>stationary</i> Cavity thickness: 4.0 mm	
Comp. 4-1 mm	Linear motion Linear mode: <i>compression</i> Initial cavity thickness: 4.0 mm Final cavity thickness: 1.0 mm Linear time: 3.5 s Overall time: 43.5 s	
Exp. 1-4 mm	Linear motion Linear mode: <i>expansion</i> Initial cavity thickness: 1.0 mm Final cavity thickness: 4.0 mm Linear time: 7.5 s Overall time: 77.5 s	
CompR300	Linear motion Linear mode: <i>compression</i> Initial cavity thickness: 4.0 mm Final cavity thickness: 1.0 mm Linear time: 3.5 s Overall time: 43.5 s	Rotation motion Rotating mode: <i>continuous</i> Rotating speed: 300 rpm Rotating time: 3.5 s
ExpR300	Linear motion Linear mode: <i>expansion</i> Initial cavity thickness: 1.0 mm Final cavity thickness: 4.0 mm Linear time: 7.5 s Overall time: 77.5 s	Rotation motion Rotating mode: <i>continuous</i> Rotating speed: 300 rpm Rotating time: 7.5 s

- *Stationary*: the plate cavity is fixed to obtain discs with 1.0 and 4.0 mm of thickness.
- *Compression*: the plate cavity moves linearly during filling from 4.0 mm to 1.0 mm of thickness (corresponding to a compression velocity of 0.9 mm/s).
- *Expansion*: in this case the plate cavity moves linearly during filling from mm 1.0 to 4.0 mm of thickness (corresponding to an expansion velocity of 0.4 mm/s).
- *Compression combined with continuous rotation at 300 rpm*: the plate cavity moves linearly from 4.0 mm to 1.0 mm during filling under combined continuous rotation at 300 rpm (the rotating time is 3.5 s corresponding to a total of 17.5 revolutions during filling).
- *Expansion combined with continuous rotation at 300 rpm*: the plate cavity moves linearly from 1.0 mm to 4.0 mm during the injection time under continuous rotation at 300 rpm (the rotating time is 7.5 s corresponding to a total of 37.5 revolutions during filling).

Mechanical characterization

Sample preparation

For every moulding condition, specimens for tensile, flexural and impact tests were machined out from the moulded discs at the locations marked in Figs. 2 and 3, along the disc radius in the RD and transversal directions (TD).

The microstructure, fracture surfaces of the broken tensile tests and the fibre orientation measurements of the mouldings were already assessed in a previous study [22].

Tensile tests

The tensile behaviour was characterized in an Instron 4505 universal mechanical testing machine, at a constant crosshead velocity of 10 mm/min (corresponding to a nominal strain-rate of $8.33 \times 10^{-3} \text{ s}^{-1}$) and in a controlled environment (23 °C and 55% RH). At least eight samples per condition were tested. The

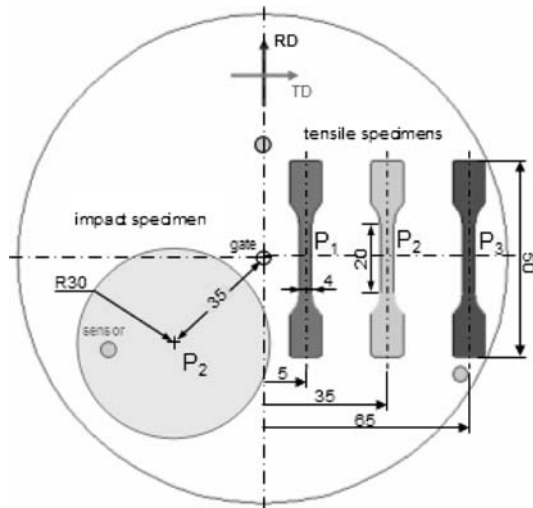


Fig. 2 Specimens for tensile and impact tests (dimensions in millimeters)

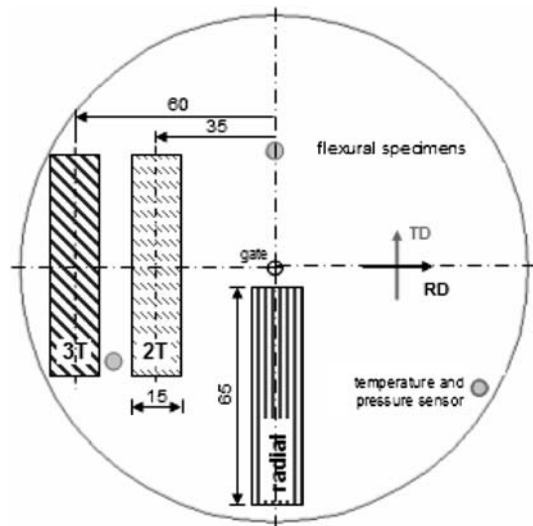


Fig. 3 Specimens for flexural tests (dimensions in millimeters)

mechanical properties studied were the tensile initial modulus (E), the maximum stress (σ_{\max}), the strain at break (ϵ_b) and the energy at break (U_b).

Flexural three-point bending tests

Three-point support bending tests were carried out on an Instron 4505 universal mechanical testing machine for determining the flexural modulus of the specimens, E_f . The flexural bars were simply supported at a span of 40 mm. The crosshead velocity used was 1.50 mm/min (corresponding to nominal strain-rates at the outer fibre of 5.63×10^{-3} and $2.52 \times 10^{-2} \text{ s}^{-1}$ for 1 and 4 mm thick discs, respectively), and the test environment was controlled

(23 °C and 55% RH). The flexural modulus was determined in radial and TD, respectively (Fig. 3). At least eight samples per condition were tested.

Flexural disc tests

The most typical loading situation for plate mouldings is bending. The flexural stiffness of centre gated discs can be experimentally assessed by a flexure test devised to overcome the inherent non-flatness of this type of mouldings [23]. The discs were loaded at the centre and subjected to three-point support bending tests to assess and compare their flexural stiffness, C (Fig. 4). This non-destructive test allows determining the flexural behaviour of anisotropic plates in terms of a flexural stiffness and enables the assessment of the flexural performance of anisotropic composite plates in loading situations closer to real service conditions [23, 24].

As Poisson's coefficient is unknown, the results are presented in terms of reduced flexural stiffness [23], given by

$$C_R = \frac{3}{2\pi \cdot h^3} \cdot R^2 \cdot S_p \quad (1)$$

where R is the radius of the circumference where the supports are located, h is the thickness of the disc and S_p , the corrected slope, calculated as:

$$S_p = \frac{S_0}{0.59 \cdot (1 - e^{-4.1(\Delta R/2R)}) + 1} \quad (2)$$

where ΔR is the radial overhang [23].

The flexure tests were carried out on an Instron 4505 universal mechanical testing machine at a crosshead velocity of 1.5 mm/min in a controlled test environment (23 °C and 55% RH). Discs were tested with three supports located at the perimeter of a circumference of 93.5 mm diameter ($\Delta R = 28.25$ mm). The mouldings were carefully placed on the supports always with the same orientation relative to the supports. It was also ensured that the moveable mould

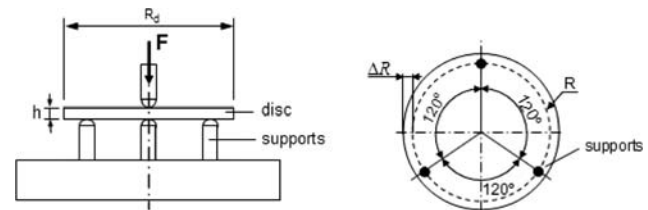


Fig. 4 Schematic diagram of the 4-point support flexural disc test

wall was always opposite to the loading point. Six discs were tested for each condition. The disc thickness was calculated as the average value of six measurements in points equally spaced in the disc periphery.

Impact tests

The impact tests were performed in an instrumented falling-weight impact test machine (Rosand IFWIT type 5) at 23 °C and 55% RH, without lubrication of the striker. A falling mass of 25 kg was used with a hemispherical striker tip of 10 mm of diameter. The striker velocity was 2 m/s. The frequencies over 3 kHz were eliminated by software using a digital filter.

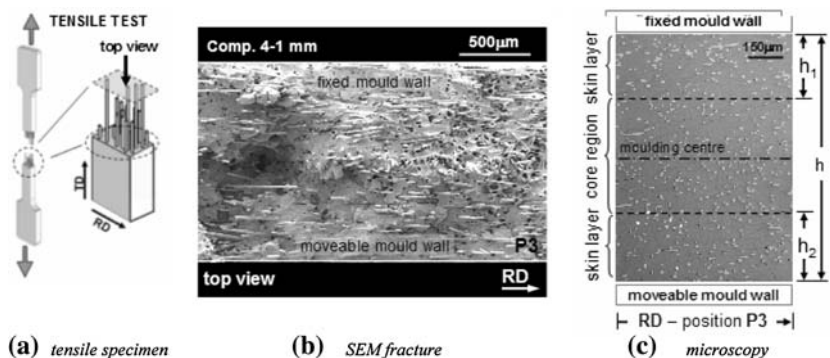
The discs were carefully placed on a circular support (with outside diameter of 60 mm), and clamped by a pneumatically actuated ring of internal diameter of 40 mm. At least eight samples per condition were tested. The disc thickness was calculated as the average value of three measurements on equally spaced points at a radius of 35 mm. The peak impact force, F_p , and the peak energy, U_p , were determined from the force-deflection curves.

Microscopic studies

The fractures surfaces of broken tensile specimens (Fig. 5a) were sputter-coated with a thin conductive layer of gold. Fractographic studies were carried out in detail on these fracture surfaces by scanning electron microscopy (SEM), using a Leica Cambrigde equipment LS360. Figure 5 depicts the position of the specimen relatively to RFD and the correspondent SEM micrographs (Fig. 5b). This analysis was complemented with reflection polarized light microscopy [22] in order to assess the morphology of the mouldings (Fig. 5c) and to compute the core ratio, defined as:

$$\%core_ratio = \frac{h - (h_1 + h_2)}{h} \times 100 \tag{3}$$

Fig. 5 Fracture surfaces from tensile specimens observed by SEM and microscopy observations



Results and discussion

Morphology of the mouldings

The fibre orientation states in a composite can be statistically evaluated by an orientation distribution function [11, 25] describing the probability of finding fibres with a given orientation relatively to a predefined direction. Tucker and co-workers have proposed the use of tensors to describe and predict fibre orientation in injection moulding [25]. Following the methodology adopted by Tucker and Advani [11], the orientation of a single fibre in a short fibre composite can be defined by two angles (θ , ϕ) of a unit vector p oriented along the main fibre axis as shown in Fig. 6. The Cartesian components of vector p on the reference coordinate system are given in Fig. 6.

The fibre orientation was evaluated in terms of the a_{22} second-order tensor component, representing the orientation in TD [25]. Details on the experimental assessment of a_{22} may be found elsewhere [22].

Figures 7 and 8 compare the evolution of the a_{22} second-order tensor component through the moulding thickness for stationary, compression and expansion mouldings at position P3 (the location where more

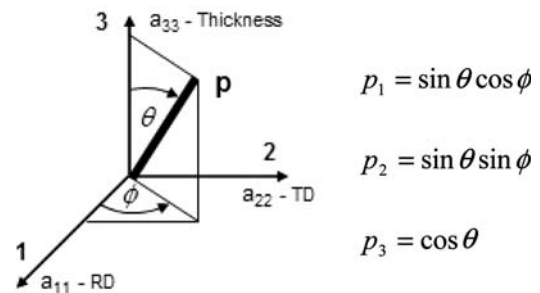


Fig. 6 Definition of the co-ordinate system used, the in-plane angle ϕ , the out of the plane θ and the unit vector p . The directions 1, 2 and 3 refer to radial, transverse flow and thickness directions, respectively

significant variations were found, due to the more pronounced effects of the rotating actions).

The a_{22} values in the middle and skins regions correspond to the local orientations measured in the centre of the mouldings and in the layer close to the mould walls, respectively. The average orientation a_{22} value was calculated as weighted average over the total thickness of the mouldings.

The linear and the rotation motions imposed by the RCEM affect the fibre orientation through the moulding thickness as shown in Figs. 7 and 8, and can be found in detail elsewhere [22]. The imposed rotation action during the filling stage leads to fibres highly oriented in TD through whole the moulding thickness. This effect is more pronounced in the skin layers, especially in the skin close to the moveable mould wall (comparatively to the stationary moulding condition the fibre orientation increases around 76% and 110%

for mouldings obtained by compression and expansion under continuous rotation, respectively). The SEM micrographs (Figs. 7, 8) confirm the measured fibre orientation profile: the majority of the fibres in the core zone are oriented perpendicular to RD. For the stationary conditions the fibres are more randomly oriented with many fibres lying parallel to RD. However, the increase of fibre alignment with the compression and expansion motions can be noticed, especially when a rotation action is simultaneously combined: fibres tend to be highly aligned in TD as a result of the imposed rotation action.

Figure 9 shows the core ratio of the mouldings at position P3 as a function of the linear and rotation motions. This ratio was calculated from polarized light microscopy photographs [22]. As expected, the core thickness significantly increases when the rotation motion is combined with the linear movements

Fig. 7 Variation of the a_{22} second-order tensor component through the moulding thickness and SEM micrographs of fracture surfaces of compression injection mouldings (broken tensile specimens), at position P3

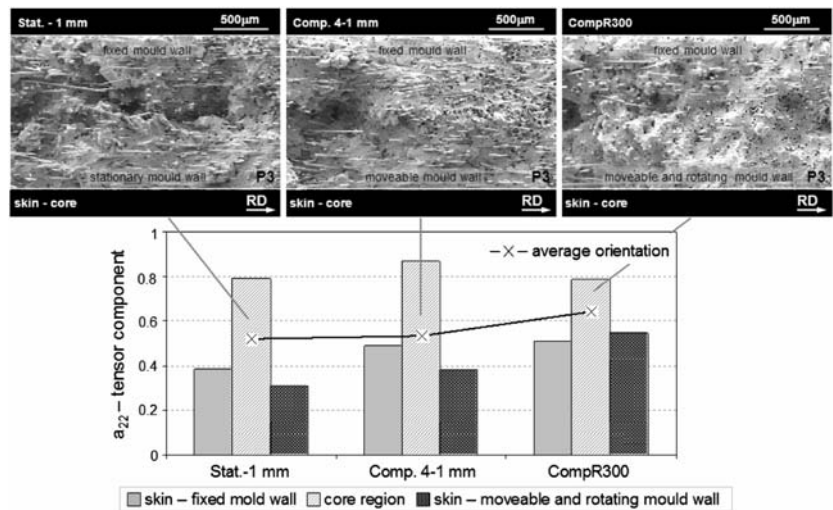


Fig. 8 Variation of the a_{22} second-order tensor component through the moulding thickness and SEM micrographs from the centre of fracture surfaces of expansion injection mouldings (broken tensile specimens), at position P3

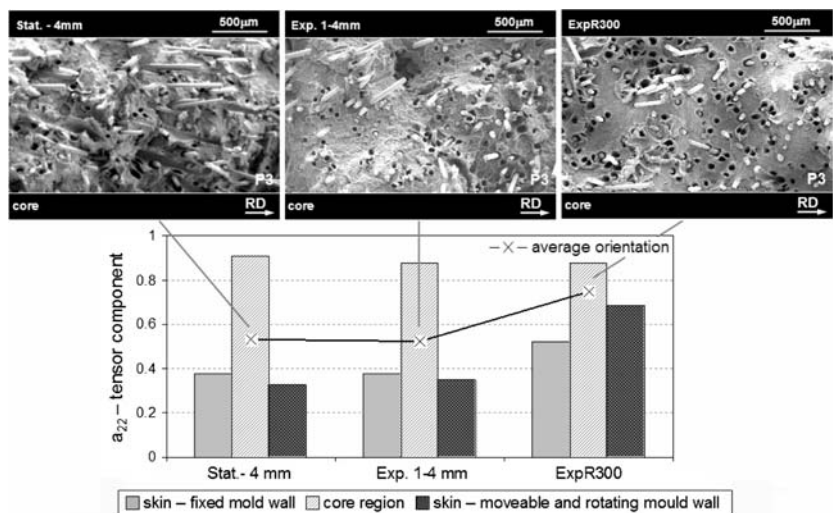
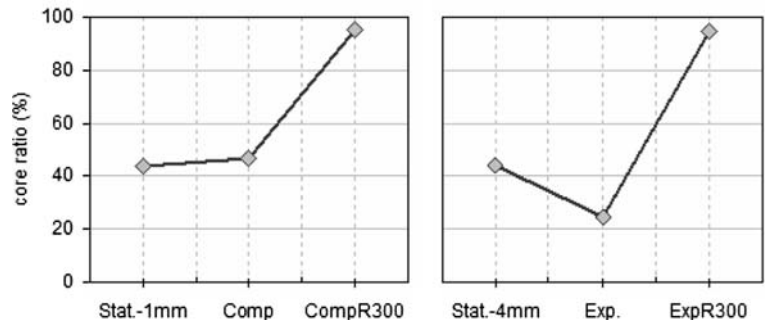


Fig. 9 Variation of the core ratio at position P3 for all injection moulding conditions



(CompR300 and ExpR300). However, for the expansion motion the core ratio slightly decreases comparatively to the stationary condition.

Figure 10 presents the dependence of the \bar{a}_{22} averaged orientation with the core ratio. The figure shows that the \bar{a}_{22} increases linearly with core ratio, being obtained a good agreement. This means that more fibres are oriented in TD as the core ratio increases.

Mechanical behaviour

Tensile tests

The typical stress versus strain curves obtained on the tensile experiments for all moulding conditions at position P3 are shown in Fig. 11. A similar brittle-ductile behaviour was observed for the others positions for all moulding conditions. The mouldings obtained with continuous rotation motion exhibit higher values of modulus and strength. However, the strain at break only varies slightly. The average experimental error on the measurements of E , σ_{max} , ϵ_b and U_b was of 3.3%, 2.1%, 3.3% and 5.2%, respectively.

Figures 12–15 present the dependence of the tensile properties on the linear and rotation motion modes of the mould surface along the flow path. Figure 12 shows

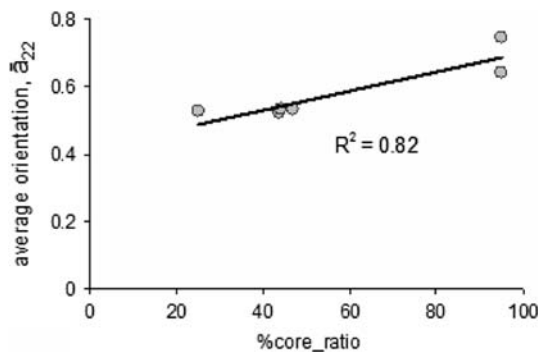


Fig. 10 Variation of average orientation (\bar{a}_{22}) with core ratio at position P3. The solid line is a best fit to the experimental points ($\bar{a}_{22} = 0.0028 \cdot \%core_ratio + 0.42$)

the variations of E along the flow path as a function of motion modes of the mould surface. For the thinner mouldings (compression mode) there are no significant variations on E ($\Delta E = 1.3\%$) along the flow path. However, the evolution is significantly different when a rotation action is imposed during filling, which leads to a pronounced difference on the tensile modulus along the flow path of 32%. This effect evidences that fibres are strongly oriented transversely to RD at position P3 as already reported [22], which is also the direction of the applied load in the tensile test. This influence is more pronounced far away from the gate (position P3) than near to the gate (position P1).

For the thicker mouldings (expansion mode) it was observed a slight increase on E along the flow path. However, when they are compared with the previous ones, the decrease of the stiffness of the specimens cut, far away from the gate (position P3) is noticeable due to lower values of the core ratio (Fig. 9). When a rotation action is imposed during the filling stage, the evolution of the tensile modulus is again significantly different: the values of E are 20% higher for position

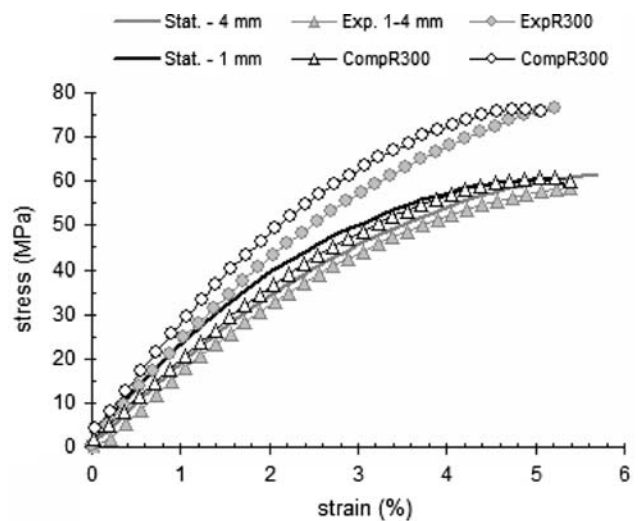
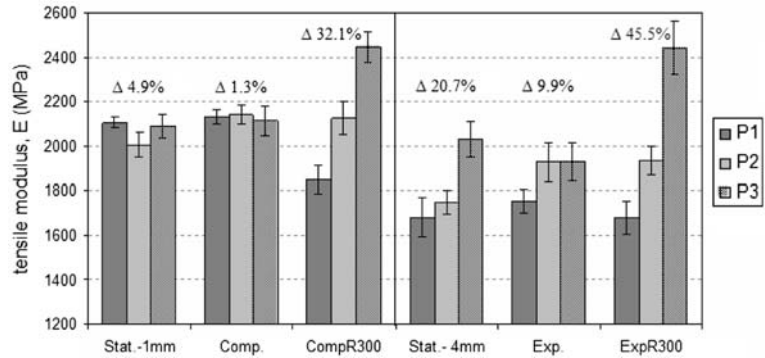


Fig. 11 Tensile stress versus strain curves (at position P3) for all injection moulding conditions

Fig. 12 Variations on the tensile modulus for all injection moulding conditions, Δ is the variation along the flow path ($\Delta = (\text{max.} - \text{min.}) / \text{min.} \times 100$)



P3 than the ones observed for the stationary mode. A pronounced difference of the tensile modulus along the flow path is also noticed showing variations up to 46%. These results also confirm that fibres are strongly oriented transversely to RD (which is also the direction of the applied load in the tensile test) as already reported [22].

The thinnest mouldings exhibit significantly higher E values than those observed for thicker mouldings. This may be attributed to the high alignment of the fibres and the matrix polymer throughout the whole thickness caused by higher shear rates developed in this case. In spite of the expansion mouldings exhibiting similar average orientation comparatively to the compression ones, they have a pronounced reduction of the core ratio and lower values of orientation (a_{22}) in the skin layers. In fact, the tensile modulus depends on the orientation profile through the thickness (while the bending modulus could well be more sensitive to differences in the skin orientation level).

Figure 13 shows the variations of the maximum stress, σ_{max} for the three locations along the flow path as a function of motions modes of the mould surface. These variations are similar to those found for the tensile modulus. The higher σ_{max} values are found for the linear motion combined with rotation action modes at position P3. These mouldings also show the higher variation of σ_{max} along the flow path.

Fig. 13 Variations on the maximum stress for all injection moulding conditions, Δ is the variation along the flow path ($\Delta = (\text{max.} - \text{min.}) / \text{min.} \times 100$)

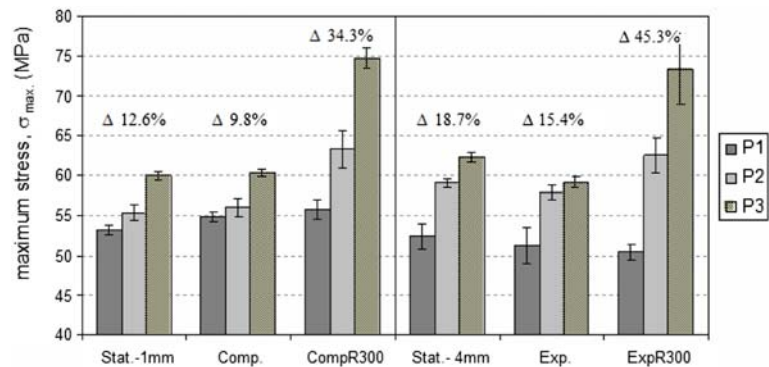


Figure 14 shows the variations of the elongation at break, ϵ_b for all moulding conditions. The compression with or without rotation motions induced by the RCEM do not affect significantly the material ductility. This behaviour seems to evidence that the fracture is dictated by the matrix response, which is affected by the presence of fibres but not by the respective level or pattern of orientation. Furthermore, the thickest moulding exhibit higher ϵ_b values than those observed for thinner mouldings. However, when the expansion mode is imposed, ϵ_b slightly decreases: this is more evident at position P3.

On the other hand, the energy at break (Fig. 15) slightly increases for compressed mouldings but decreases for expanded ones. In the former case this effect is more pronounced when the rotation motion is imposed: the variation along the flow path increases, to around 20% for the CompR300. In the case of expansion mode, imposing rotation increases the energy at break at positions P2 and P3, while still a small decrease at P1 is noticed.

Flexural three-point bending tests

In a tensile test, the entire cross-section is almost subjected to the same level of loading, whereas in flexural mode the external layers are highly loaded. When the material is inhomogeneous and anisotropic,

Fig. 14 Variations on the strain at break for all injection moulding conditions, Δ is the variation along the flow path ($\Delta = (\text{max.} - \text{min.}) / \text{min.} \times 100$)

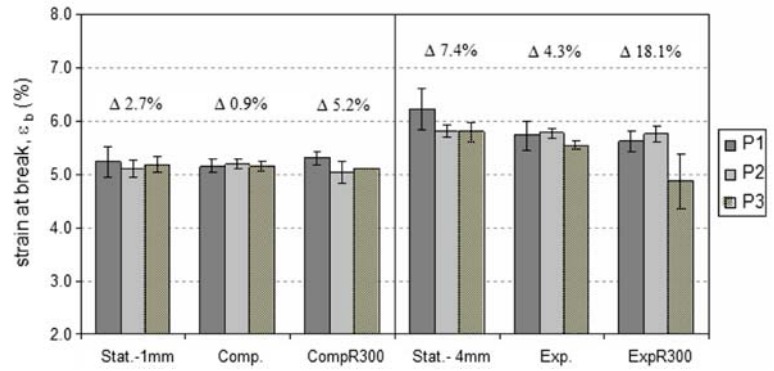
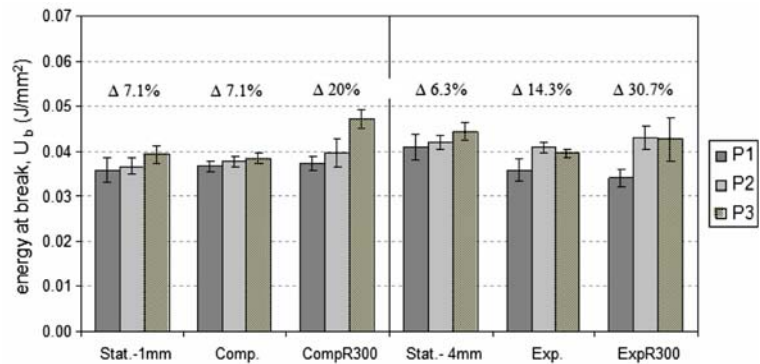


Fig. 15 Variations on the energy at break for all injection moulding conditions, Δ is the variation along the flow path ($\Delta = (\text{max.} - \text{min.}) / \text{min.} \times 100$)



it is very likely that the modulus measured in tensile and flexure will differ significantly due to differences in the fibre orientation distribution in the skin and core regions [1].

In the three-point flexural test, the response of the mouldings is largely influenced by the properties of the skin layer opposite to the point loading, which is in our case the skin zone of the moveable mould wall. Figure 16 shows the flexural modulus values obtained in radial and transversal flow directions as a function of the motion modes of the mould surface. The average experimental error on the measurements of E_f is 4.6%.

These data show that E_f is very sensitive to the fibre orientation. In stationary conditions there is no

significant property difference between the behaviour in RD and the TD direction. However, this changes for compression and expansion modes, which results in mouldings with a pronounced level of anisotropy, with an increasing of 12% for linear motions—Comp and Exp and of 40% for linear motions combined with rotation motion—CompR300 and ExpR300, respectively, as shown in Table 2.

Compression and expansion modes induce a slight increase on the flexural modulus in radial direction compared to stationary mode, because most of the fibres tend to lie parallel to RD. In compression modes the thickness of the skin layer increase due to the linear motion of the cavity plate from greater to smaller

Fig. 16 Effects on the flexural modulus for all injection mouldings conditions

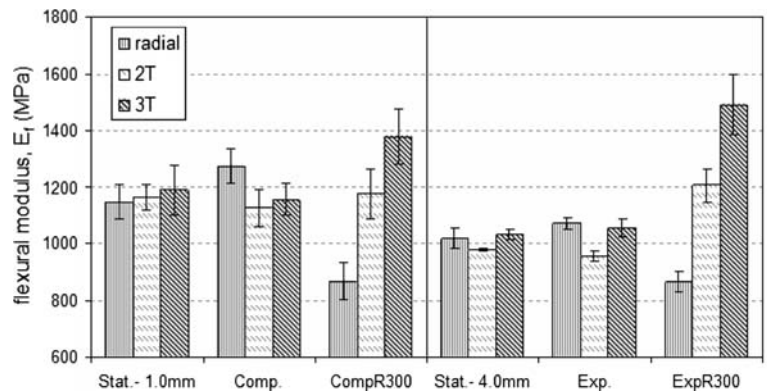


Table 2 Percent variation of the anisotropy (between E_f (radial) and E_f (2T))

Stat.-1 mm	Comp	CompR300	Stat.-4 mm	Exp.	Exp300
+1.5	-11.8	+35.5	-3.9	-10.7	+39.1

$$\% \text{anisotropy} = \frac{E_f(2T) - E_f(\text{radial})}{E_f(\text{radial})} \times 100$$

thickness during the mould filling stage [22]. The fibres in the skin layer are predominantly aligned in RD, leading to a higher flexural modulus in the radial direction.

The effect of the rotation action during mould filling in compression or expansion modes induces an increase of the flexural modulus in the transversal direction (2T and 3T). This effect is more pronounced far away from the gate at position 3T. These variations are of 17% and 24% higher for compression and expansion mode, respectively (Table 3). This evidences that fibres are strongly oriented to TD and weakly oriented in RD, leading in comparison to the stationary condition to a decrease of 24% and 15% on the radial flexural modulus for compression and expansion mode, respectively.

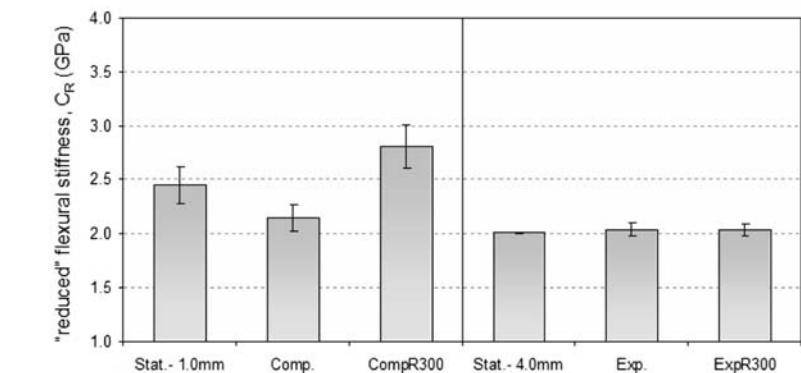
Flexural disc test

Figure 17 shows the variations of the reduced flexural stiffness, C_R of a centre gated discs as a function of motion modes of the cavity plate. The average experimental error of C_R is 4.3%. From the Fig. 17 can be seen

Table 3 Percent variation of the flexural modulus along the flow path (between 2T and 3T position)

Stat.-1 mm	Comp	CompR300	Stat.-4 mm	Exp.	Exp300
+2.3	+2.5	+17.4	+5.6	+10.4	+23.8

$$\% \text{var.} = \frac{E_f(3T) - E_f(2T)}{E_f(2T)} \times 100$$

Fig. 17 Effects on the reduced flexural stiffness for all injection mouldings conditions

that the expansion motion of the mould cavity does not affect the flexural stiffness of the discs. On the other hand for compression mouldings there is a decrease in the flexural stiffness. However, when the rotation motion is combined, the flexural stiffness increases, being 15% higher than in stationary mode.

Impact tests

The typical force–displacement curves of the impact test for all moulding conditions are presented in Fig. 18. A similar behaviour was observed for all moulding conditions. The peak values refer to the force and energy at the first significant peak. This is not related to the failure initiation but is associated to the formation of a major defect (transverse crack), which reduces the system compliance [26]. The results of impact peak force (F_p /mm) and peak energy (U_p /mm) were normalized with respect to the specimen thickness. The average experimental errors were 6.4% and 10.2% for F_p and U_p , respectively.

The F_p and U_p dependencies on the motions modes of RCEM are shown in Fig. 19. The differences in the measured force levels between the two sets of data are due to the different thicknesses of the mouldings (4 and 1 mm of thickness, respectively). For all conditions, the impact properties show a small decrease with the linear motions of the mould cavity. However, a non-negligible variation was observed for expansion mode with rotation leading to a decrease of 12% and 17% on the impact peak energy and peak force, respectively. The expansion mouldings under continuous rotation show the fibres highly oriented transversely to RD and weakly oriented in the radial direction [22].

The reduction of the impact properties with the fibre orientation indicates a negative effect of fibre orientation anisotropy on the multi-axial impact performance. Besides, an additional effect of fibre breakage due to the rotation action may be present. This is

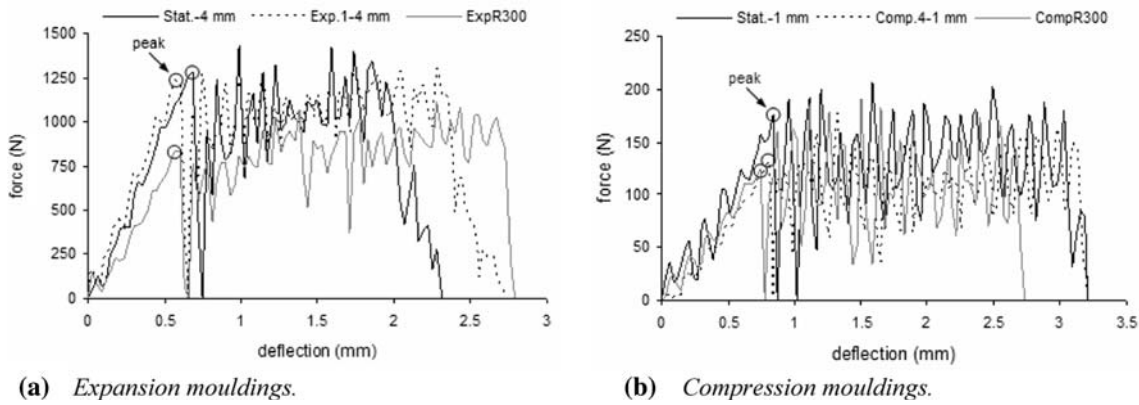
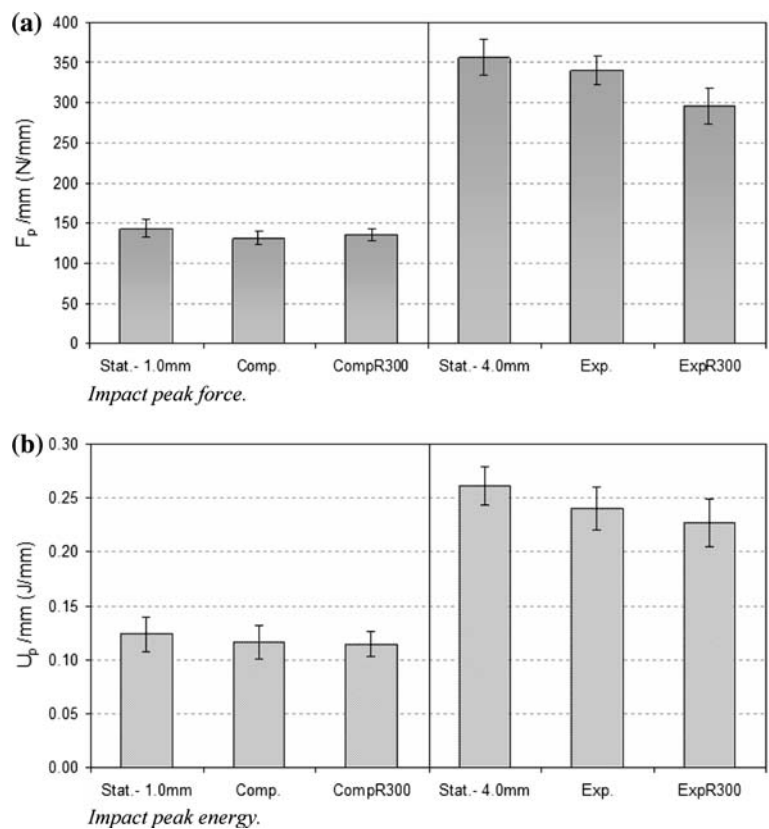


Fig. 18 Falling-weight tests—force versus deflection plot (no filtering) for all injection moulding conditions

Fig. 19 Effects of the impact peak force and energy for all mouldings conditions

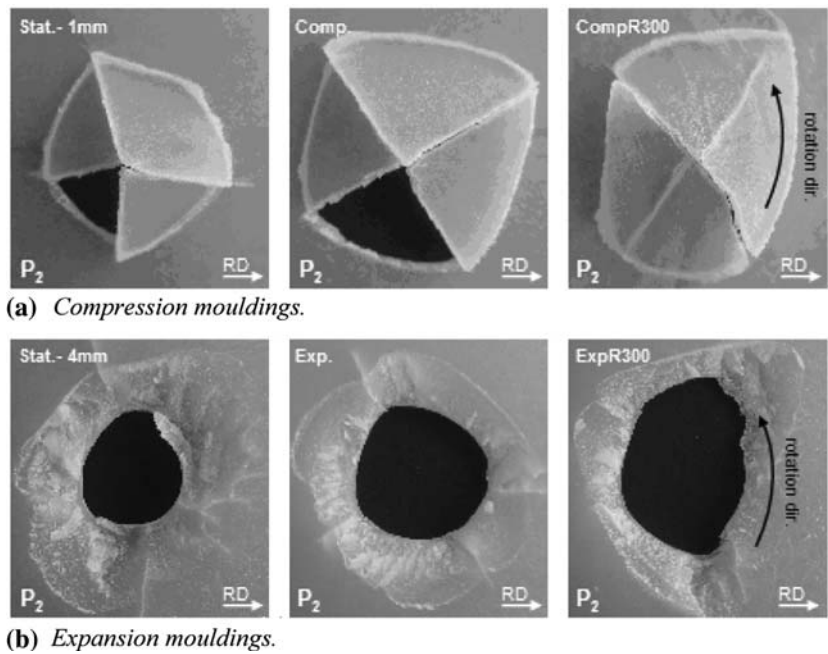


subject of a future detailed study on the effect of the linear motions of the cavity on the fibre length degradation and subsequent mechanical properties. In the falling-weight test the loading is multi-axial i.e. the direction of failure is not imposed and a crack can propagate in the weakest direction [27]. Any anisotropy present, such as excessive orientation in one direction, leads to weakness in this direction as crack easily growth. When the load is applied perpendicular to the fibres, good adhesion is required for even moderate impact resistance. For that reason in our

mouldings once the crack is initiated, the presence of fibres can not hinder its propagation because of low energy absorbing mechanisms, such as fibre debonding and fibre pullout [2].

Figure 20 shows the photographs of the impact fracture surfaces for each mouldings condition. For the thicker mouldings, the stationary mouldings failed at much higher impact force and energy (Fig. 19) with cracks in several directions that is typical behaviour of non-oriented moulded parts. On the other hand, for the expansion and compression under continuous

Fig. 20 Photographs of the impact fracture surfaces for all moulding conditions



rotation conditions (ExpR300 and CompR300), the cracks have a preferential direction, which coincides with that of the fibres. This effect is more pronounced for the expansion mouldings.

Mechanical properties versus fibre orientation

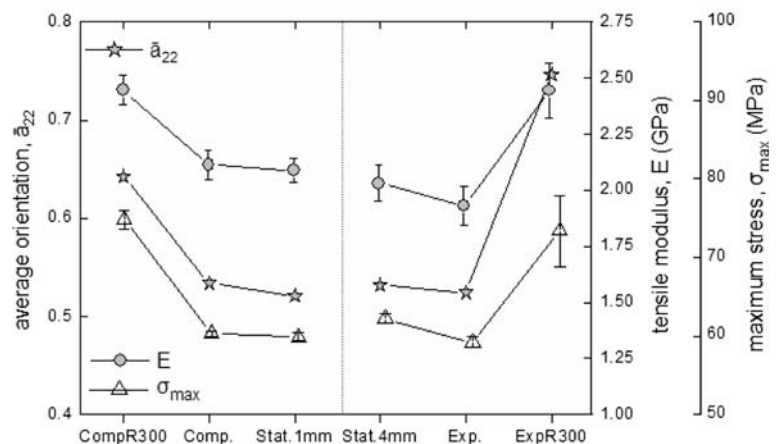
The tensile and flexural three-point bending properties were related with the \bar{a}_{22} average orientation. These relationships were obtained by fitting the experimental data to linear equations. The goodness of the fits is evaluated by the higher values of the coefficient of multiple regressions, R^2 . The mechanical properties and the microstructural characterization were performed at the same location (P3 and 3T, for tensile and flexural tests respectively). As the

mechanical properties are dependent upon the fibre orientation and the thickness of oriented layers, the effect of the former was weighted by the amount of material oriented in that direction. A microstructural parameter was then defined as $\bar{a}_{22} \cdot \% \text{core_ratio}$, assuming that the mechanical response in the TD is directly related to the skin/core ratio and respective properties.

Tensile properties

Figure 21 shows that σ_{max} and E increase both with \bar{a}_{22} , being confirming a good agreement between the variations of \bar{a}_{22} and the mechanical properties. Figure 22 shows the relationship between E and σ_{max} with $\bar{a}_{22} \cdot \% \text{core_ratio}$ (R^2 values are of 0.98 and 0.97,

Fig. 21 Tensile modulus and maximum stress versus \bar{a}_{22} -average orientation at location P3



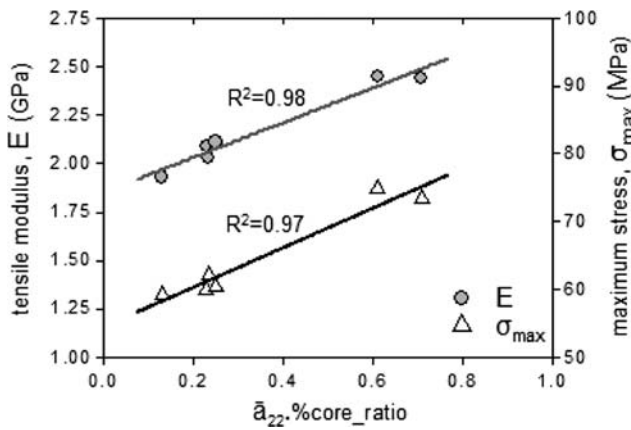


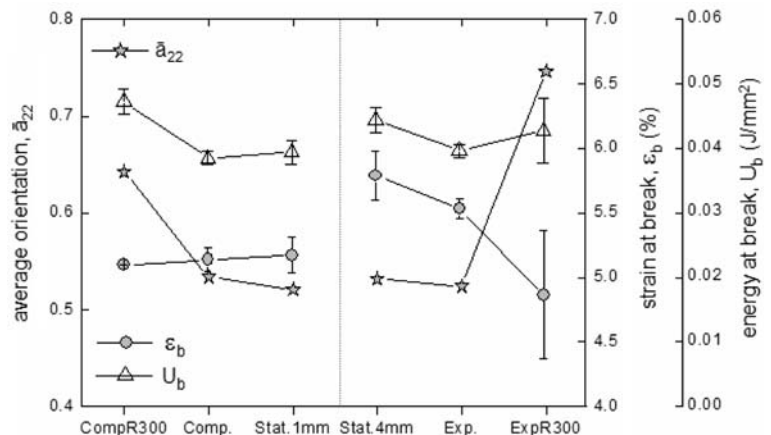
Fig. 22 Fitting of the experimental values for tensile modulus and maximum stress versus $\bar{a}_{22} \cdot \%core_ratio$ at location P3. The solid lines are the best fit to the experimental points for tensile modulus and maximum stress, $E = 1.85 + 0.90 \cdot (\bar{a}_{22} \cdot \%core_ratio)$ and $\sigma_{max} = 54.45 + 29.20 \cdot (\bar{a}_{22} \cdot \%core_ratio)$, respectively

respectively). The results confirm the findings by other authors [1, 2, 5], that the stiffness and the strength of a short fibre reinforced thermoplastic are directly dependent on fibre orientation and amount of oriented matrix.

Figure 23 shows the variation of ϵ_b , U_b and \bar{a}_{22} with the motion action of the mould surface. ϵ_b decreases for higher values of \bar{a}_{22} for the expansion mouldings. Whereas U_b follows the same trend as the average orientation values, increasing with higher values of \bar{a}_{22} .

For these properties no good fitting was obtained for the relationships between them and $\bar{a}_{22} \cdot \%core_ratio$. In spite of the higher experimental error generally associated to these properties, this may indicate that other microstructural parameter should be considered for correlation with property at break.

Fig. 23 Tensile strain and energy at break versus \bar{a}_{22} -average orientation at location P3



Flexural three-point bending properties

Figure 24 shows the relationship between the flexural modulus in the transversal direction (at location 3T) and \bar{a}_{22} as a function of motion modes. As expected, the E_f tends to increase with \bar{a}_{22} , being noticeable the good agreement. Figure 25 shows the relationship between E_f with $\bar{a}_{22} \cdot \%core_ratio$. The high value of the coefficient of multiple regression, $R^2=0.96$, confirms the important dependencies of E_f on fibre orientation and amount of oriented material in TD.

Conclusions

The current work shows that the RCEM mould produces preferential orientation of the short glass fibres in the polypropylene matrix, which is reflected in the mechanical properties of the mouldings.

- The compression and expansion modes produce no significant differences in the average fibre orientation level compared to the stationary mode.
- The use of the rotation motion imposed during the filling in compression or expansion modes induce a property variation along the flow path. Far away from the gate the effect of the rotation is stronger, which is reflected in the orientation of the fibres, highly aligned transversely to the RD direction.
- Compression and expansion modes combined with continuous rotation action increase the tensile modulus and yield stress in transverse direction. However, no significant effect was noticed in the elongation and energy at break.
- Compression and expansion combined with continuous rotation increase the flexural modulus in the transversal direction. However compression moulding

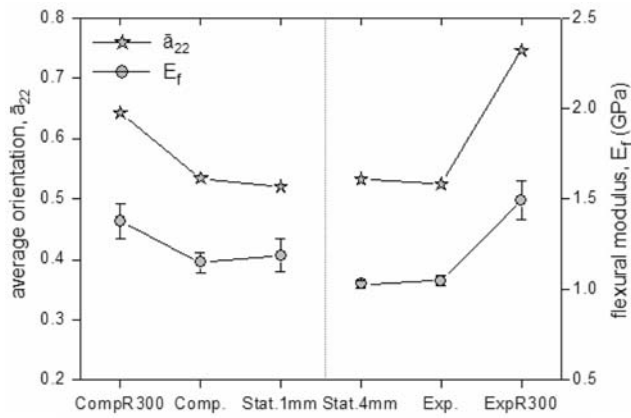


Fig. 24 Transversal flexural modulus versus \bar{a}_{22} -average orientation at location 3T

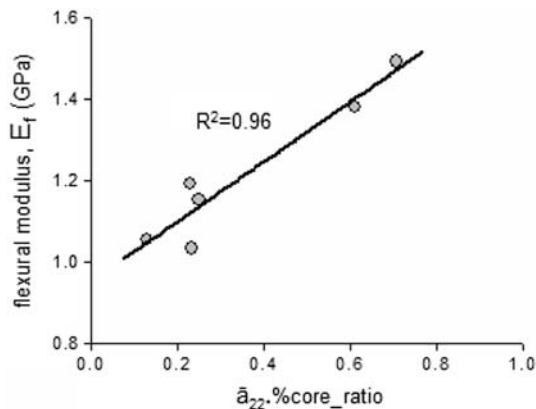


Fig. 25 Fitting the experimental values for flexural modulus versus $\bar{a}_{22} \cdot \% \text{core_ratio}$ at location 3T. The solid lines is a best fit to the experimental points $E_f = 0.95 + 0.73 \cdot (\bar{a}_{22} \cdot \% \text{core_ratio})$

dings only increase flexural modulus in the radial direction.

- The flexural stiffness of the injection-moulded part does not depend significantly on the linear motion; however the flexural stiffness slightly increases for the compression under continuous rotation. This was attributed to the increase of the fibre orientation caused by the rotation motion imposed.
- The impact behaviour of the injection-moulded part does not depend significantly on the linear motion; however a slight decrease of the strength is observed for highly oriented mouldings as does fibre obtained when the rotation mode is used.

The use of the rotation motion imposed during the filling process leads to increase fibre alignment greatly

affecting the parts mechanical properties. The micromechanics of these phenomena will be discussed in a subsequent paper.

Acknowledgements The authors are indebted to the Portuguese Foundation for Science and Technology for the financial support received, under frame of 3rd European Framework Program, POCTI and FEDER programs.

References

- Folkes MJ (1982) Short fibre reinforced thermoplastics, Research Studies Press, John Wiley and Sons Ltd
- Nielsen LE Mechanical properties of polymers and composite, vol 2. Marcel Dekker Inc., New York
- Neves NM, Pouzada AS (1999) J Inject Moulding Technol 3:3
- Xia M, Hamada H, Maekawa Z (1995) Int Polym Process 10(1):74
- Joshi M, Maiti SN, Misra A, Mittal RK (1994) Polym Comp 15:5
- Doshi SR, Charrier J-M (1989) Polym Comp 10:1
- Yu Z, Brisson J, Ait-Kadi A (1994) Polym Comp 15:1
- Hine PJ, Duckett RA, Ward IM, Allan PS, Bevis MJ (1996) Polym Comp 17(3):400
- Singh R, Chen F, Jones FR (1998) Polym Comp 19(1):37
- Neves NM, Isdell G, Pouzada AS, Powell PC (1998) Polym Comp 19(5):640
- Tucker III CL, Advani SG (1994) In: Advani SG (Ed) Flow and rheology in polymer composites manufacturing. Elsevier, Amsterdam, p 147
- Bay RS, Tucker III CL (1992) Polym Comp 13(4):317
- Gupta M, Wang KK (1993) Polym Comp 14(5):367
- Verweyst BE, Tucker III CL (2002) The Can J Chem Eng 80:1093
- Verweyst BE, Tucker III CL, Foss PH (1997) Intern Polym Process 7:238
- Neves NM, Pontes AJ, Pouzada AS (1999) 2nd ESAFORM 341
- Bay RS, Tucker III CL, Davis RB (1989) ANTEC-89 Tech. Papers, 539
- Silva CA, Viana JC, Cunha AM (2002) PPS-18 Tech. Papers, 467
- Silva CA, Viana JC, Cunha AM (2003) PPS-19 Tech. Papers, 1076
- Silva CA, Viana JC, Cunha AM (2004) PPS-20 Tech. Papers, 198
- Silva CA, Viana JC, Dias GR, Cunha AM (2005) Int Polym Process 20:27
- Silva CA, Viana JC, van Hattum FWJ, Cunha AM (2006) Polym Comp 27(5):539
- Nunes JP, Pouzada AS, Bernardo CA (2002) Polym Test 21:27
- Pouzada AS, Stevens MJ (1984) Plast Rubber Process Appl 4:181
- Advani SG, Tucker III CL (1987) J Rheol 31:751
- Reed PE (1992) Plas Rubb Comp Proc Appl 17(3):157
- Perkins WG (1999) Polym Eng Sci 39:12